A NEW WALL FUNCTION STRATEGY FOR FORCED AND MIXED CONVECTION

T.J. Craft, A.V. Gerasimov, H. Iacovides, B.E. Launder, C. Robinson
Department of Mechanical Engineering, UMIST
P.O. Box 88, Manchester, UK

ABSTRACT

The paper describes progress in developing a wall function strategy to enable CFD predictions of turbulent convective heat transfer to be made without incurring the cost of a very fine near wall grid. Analytical expressions are obtained for the variation of velocity and temperature across the near-wall sublayer, allowing one to compute the effective "resistance" of the viscous sublayer to heat and momentum transport. The present work significantly extends the approach employed in conventional wall functions, by accounting for the effects of buoyancy, pressure gradients, convection and variations in molecular transport properties. The scheme is applied to the problems of forced and mixed convection in a vertical pipe, separated flow in an asymmetric diffuser, and to the opposed wall jet with encouraging results.

INTRODUCTION

The usual modelling practice in the application of CFD to real industrial problems is to adopt a two-equation linear eddy-viscosity model in the main region of the flow and a set of overall resistance laws or 'wall functions' to bridge the very thin region immediately adjacent to any wall that may be present. This latter practice avoids the need to resolve with a very fine grid the viscous sublayer and 'buffer' regions across which there is a rapid – and very complex – changeover from molecular to turbulent transport mechanisms. Indeed, resolving in detail the near-wall sublayer may, depending on the problem and the type of numerical solver employed, raise computation times from three to more than ten times that which would be needed with wall functions. The motivation for retaining wall functions is thus very clear.

Yet, the fact remains that the wall functions in actual use in current commercial software are based on presumed velocity variations that only pertain in simple shear flows subject to a uniform shear stress equal to that at the wall. The actual circumstances where one would like to make CFD computations are, however, far removed from this idealized state.

In fact, at the dawn of CFD for turbulent flows, the group from Imperial College were well aware of some of the factors causing departures from equilibrium behaviour and proposals were made for accommodating these effects: Spalding (1967), Patankar & Spalding (1972), Wolfshtein (1969). However, these proposals fell into disuse partly because, as the execution speeds of computers rose, researchers preferred to extend the detailed numerical solution all the way to the wall, employing what are termed 'low-Reynolds-number' models. Moreover, these 'generalized' wall functions also failed to account for the thickening of the viscous sublayer that was known to occur when the shear stress decreased significantly across the sublayer: laminarization or re-laminarization as it is termed. Simple log-law wall functions – while also not reproducing this phenomenon – usually do less badly.

From the heat-transfer point of view, it must also be said that none of the above-cited works considered natural convection. While George and his co-workers (see George & Capp, 1979) have discussed the limiting form of a wall function for natural convection on a vertical flat plate, the proposed scaling is not suitable for use in the more common mixed-convection situation where buoyant action is a contributor to, rather than the only factor driving fluid motion.

The present work has been motivated by the need to undertake CFD predictions of complex heat transfer plant under mixed convection. Our attention has been limited to vertical surfaces where it is well known, Cotton & Jackson (1987), that the low-Reynolds number k-ε model does especially well in capturing the suppression of Nusselt number that may arise in situations where buoyant motion aids the forced motion. Our aim has been to develop a wall-function scheme capable of mimicking that predicted by the model. Length limitations mean that not all the equations can be cited in full in the present work. Somewhat more detail

is available in Craft et al (2001) while a technical report, Gerasimov (2001), provides a complete statement. It is emphasized that these are not just mixed-convection wall functions. They have been applied to forced-convection, including situations where the molecular transport properties are highly temperature dependent, and to the velocity field in separated flow in a diffuser. In all cases considered significant improvement is achieved over the log-law form for an insignificant increase in execution time.

The following sections provide an outline of the analysis and consider applications covering both buoyancy affected and purely forced-convection situations. Finally, the concluding section considers briefly further developments of the methodology.

THE NEAR-WALL MODEL

Preliminaries

The treatment is developed within a finite-volume numerical discretization of the flow. Figure 1 shows the near-wall control volume whose west boundary coincides with the wall, with the cell node at P. The viscous sublayer extends to a distance y_v from the wall and, initially, we assume that y_p (the value of normal coordinate at node P) is greater than y_v. The turbulent viscosity is taken as zero within the viscous layer and for $y > y_v$ is assumed to increase linearly with distance from the edge of the sublayer:

$$\mu_t = c_\mu c_l (y^* - y_v^*)\mu_v \qquad (1)$$

The constants c_μ and c_l are those conventionally adopted in 1-equation eddy viscosity models (0.09 and 2.55) while y^* is the dimensionless wall distance $\rho_v y k_p^{1/2}/\mu_v$, where the subscript v denotes properties evaluated at the edge of the viscous sublayer. While Chieng & Launder (1980) proposed that k in the definition of y^* should also be evaluated at y_v, this was found to render the result more sensitive to the thickness of the wall adjacent control volume. The form adopted in eq. (1) simplifies integration, yet retains the essentials of a continuous effective viscosity curve where the turbulent viscosity is zero for a finite region next to the wall. Figure 2 suggests a uniform molecular viscosity; for flows involving a large temperature range significant variation in this property may occur across the sublayer, and modifications to account for this are described later.

Thermal Analytical Wall Function

In the case of buoyant flows the temperature enters the momentum equation as a source term and so analysis begins with the thermal field. Neglecting diffusion parallel to the wall the enthalpy transport equation may be written:

$$\rho U \frac{\partial T}{\partial x} + \rho V \frac{\partial T}{\partial y} = \frac{\partial}{\partial y}\left[\left(\frac{\mu}{\mathrm{Pr}} + \frac{\mu_t}{\mathrm{Pr}_t}\right)\frac{\partial T}{\partial y}\right] \qquad (2)$$

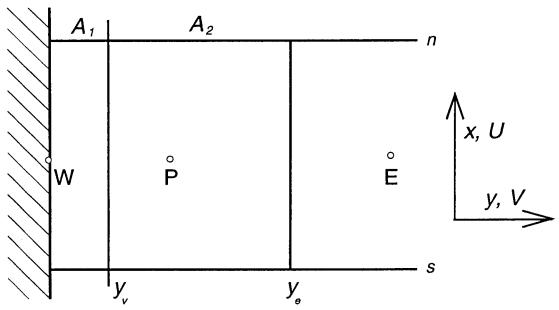

Figure 1: Near-wall control volume.

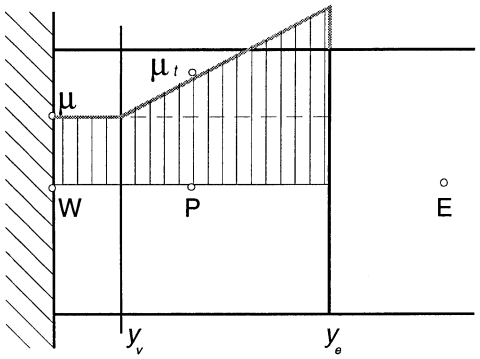

Figure 2: Assumed turbulent viscosity variation.

or, in y^* coordinates:

$$C_{th} \equiv \frac{\mu_v^2}{\rho_v^2 k_p}\left(\rho U \frac{\partial T}{\partial x} + \rho V \frac{\partial T}{\partial y}\right) = \frac{\partial}{\partial y^*}\left[\left(\frac{\mu}{\mathrm{Pr}} + \frac{\mu_t}{\mathrm{Pr}_t}\right)\frac{\partial T}{\partial y^*}\right] \qquad (3)$$

The usual wall function assumptions lead to convective transport being discarded on the grounds that near the wall it is negligible in comparison with diffusive transport. In the present work different strategies for including the main elements of the convective terms have been tested, the most stable approach being to retain only the first term in non-conservative form, i.e.

$$C_{th} = \frac{\mu_v^2}{\rho_v^2 k_p}\left(\rho U \frac{\partial T}{\partial x}\right) \qquad (4)$$

Equation (3) can be integrated separately over the viscous and turbulent regions with continuity of T and $\partial T/\partial y^*$imposed at $y^* = y_v^*$, resulting in an algebraic expression for T of the form

$$T = \begin{cases} T_{wall} + \frac{\mathrm{Pr}}{\mu_v}\left[\frac{C_{th}{y^*}^2}{2} + A_{th} y^*\right] & y^* < y_v^* \\ T_{wall} + \frac{\mathrm{Pr}}{\mu_v \alpha_t} C_{th}\,(y^* - y_v^*) & \\ \quad + \frac{\mathrm{Pr}\, y_v^*}{\mu_v}\left[\frac{C_{th}}{2} y_v^* + A_{th}\right] & y^* > y_v^* \\ \quad + \frac{\mathrm{Pr}}{\mu_v \alpha_t}\left[A_{th} + C_{th}\left(y_v^* - \frac{1}{\alpha_t}\right)\right] \ln Y_T & \end{cases} \qquad (5)$$

where $\alpha_t = \mathrm{Pr}\,\alpha/\mathrm{Pr}_t$, $Y_T = [1 + \alpha_t(y^* - y_v^*)]$ and $A_{th} = -(q_{wall}/c_p)\mu_v/(\rho_v\sqrt{k_p})$.

Velocity Field Wall Function

Following a similar path to the above analysis the velocity variation in the near-wall control volume is described by

$$\frac{\partial}{\partial y^*}\left[(\mu+\mu_t)\frac{\partial U}{\partial y^*}\right] = C + b(T - T_{ref}) \quad (6)$$

where

$$C \equiv \frac{\nu^2}{k_p}\left[\rho U\frac{\partial U}{\partial x} + \rho V\frac{\partial U}{\partial y} + \frac{\partial P}{\partial x}\right] \quad (7)$$

and $b \equiv -\left(\nu^2/k_p\right)\rho_{ref} g\beta$ represents the effect of buoyancy on the mean velocity with β being the coefficient of thermal expansion.

The equation is again integrated separately across the viscous and fully turbulent regions, resulting in analytical formulations for U, which can be used to compute the wall shear stress.

In the case of buoyancy-affected flows, solution of the discretized momentum equation in the near-wall cell also requires a source term representing the average contribution of the buoyancy term across the cell. In the present approach this term is evaluated analytically by integrating the temperature profiles described above. The details of the resulting functions are omitted, due to space constraints, but are given in Gerasimov (2001).

Mean Dissipation Rate

To solve the k equation in the near-wall cell one needs to compute the average generation and dissipation rates across the cell. The former is evaluated by making use of the assumed turbulent viscosity variation and obtaining $\partial U/\partial y$ from the analytic expression for the velocity in the fully turbulent part of the cell. For the average dissipation rate we follow broadly the proposal of Chieng & Launder (1980) in assuming a 2-part dissipation profile across the wall adjacent cell. In the turbulent region the usual inverse dependence on distance is taken

$$\varepsilon = k_p^{3/2}/(c_l y) \quad (8)$$

and in the viscous layer a uniform limiting value is adopted, Jones & Launder (1972)

$$\varepsilon = 2\nu k_p/y_d^2 \quad (9)$$

However, whereas Chieng & Launder (1980) took the matching point y_d to coincide with y_v, we have continued the inverse dependence of ε with distance closer to the wall, selecting y_d such that there is no discontinuity of ε at the matching point (Figure 3):

$$k_p^{3/2}/(c_l y_d) = 2\nu k_p/(y_d^2) \quad \text{or} \quad y_d^* = 2c_l = 5.1 \quad (10)$$

The mean dissipation rate over the near-wall cell is then obtained by integrating this two-part variation to obtain

$$\overline{\varepsilon} = \frac{1}{y_e}\left[\frac{2k_p^{3/2}}{y_d^*} + \frac{k_p^{3/2}}{2.55}\ln\left(\frac{y_e}{y_d}\right)\right] \quad (11)$$

This adoption of different thicknesses for the viscous and dissipation sublayers not only brings the ε profile much closer to those obtained in DNS studies, but also improves the prediction of the log law in forced convection.

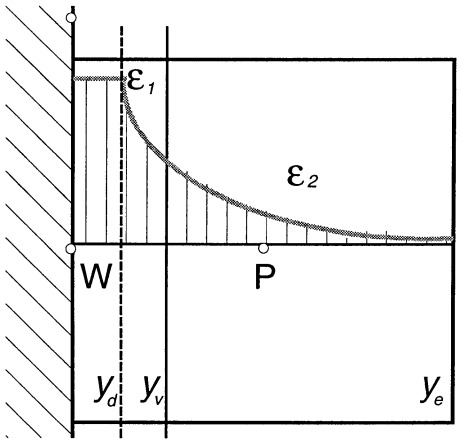

Figure 3: Modelled ε profile across the near-wall cell.

Temperature Dependence of Viscosity

In flows with significant heating some account of the variation of molecular viscosity with temperature should be made. Our initial strategy was to adopt a linear variation of viscosity over the sublayer, allowing the integration of the momentum and enthalpy equations to be still carried out. However, we were not successful in obtaining stable numerical solutions and, accordingly, the linear variation was replaced by a hyperbolic formula:

$$\mu = \frac{\mu_v}{1 + b_\mu(y^* - y_v^*)}, \quad 0 < y^* < y_v^* \quad (12)$$

where $b_\mu = (\mu_{wall} - \mu_v)/\mu_{wall}\, y_v^*$. The form chosen gave a variation of $\mu(T)$ very close to linear, allowed the analytic integration to be performed (albeit resulting in more complex expressions than eq. (5)), but avoided the stability problems.

Inclusion of Laminarization Effects

It is well established that, if the shear stress decreases rapidly with normal distance, so that the stress at the edge of the viscous layer is 10% or more below that at the wall, the viscous sublayer thickness y_v^* increases, leading to a marked reduction in Nusselt number. Many simple mixing-length and 1-equation models adopt empirical corrections making the viscous layer thickness dependent on such factors as pressure gradient or wall suction rate.

The wall-function treatment of Johnson & Launder (1982) also aimed to include such an effect. The same practice was initially followed in the present study. However, consistency requires that the turbulence energy appearing in y_v^* should be evaluated at y_v, requiring extrapolation of the values of k at y_p and y_e, a practice which was found to

be endemically unstable. Accordingly, some more stable adjustment was sought which would bring about the same effect. The practice adopted was to adjust the level of turbulence energy dissipation $\overline{\varepsilon}$ in the near-wall cell, making the factor by which the expression in eq.(11) was altered, F_ε, a function of an appropriate flow parameter. A dozen alternatives were tested but the one exhibiting least grid dependence and a satisfactory insensitivity to changes in Reynolds number was the ratio of shear stress at the edge of the viscous sublayer to that at the wall. The following was the form adopted

$$\overline{\varepsilon}_{new} = F_\varepsilon \overline{\varepsilon}_{original} \tag{13}$$

where

$$F_\varepsilon = \begin{cases} 1 + 2.25\alpha^{0.38}[1 - \exp\left(-193\alpha^2\right)] & \lambda \geq 1.02 \\ 1 & \lambda < 1.02 \end{cases} \tag{14}$$

with

$$\alpha = \left| \frac{\lambda}{1.02} - 1 \right|; \quad \lambda = \frac{\tau_{wall}}{\tau_v} = \frac{\mu_{wall}\left[(\partial U_k/\partial x_l)^2\right]^{1/2}_{wall}}{\mu_v\left[(\partial U_i/\partial x_j)^2\right]^{1/2}_{v}}$$

The correlation was arrived at by determining the values of F_ε required to bring close agreement with the low-Reynolds-number form of the k-ε model for mixed and forced convection in a pipe.

Further Refinements

The form of the wall function presented above did not (in contrast to earlier proposals) suffer greatly from grid dependence. However, when the viscous sublayer y_v occupied most or the whole of the near-wall cell two steps were found desirable. Firstly, low-Reynolds-number terms were included in the form of the k-ε model used in the external domain (beyond the wall-adjacent cells). Secondly, when y_v becomes equal to or greater than y_e, the wall functions need to be based on an analysis where the viscous region occupies all of the control volume. The details are given in Gerasimov (2001).

APPLICATIONS OF WALL FUNCTIONS

In all the cases discussed below care has been taken to ensure that the results are independent of the grid used in the main part of the flow. Further, for the cases of forced and mixed convection pipe flow, results have been obtained for a range of thicknesses of the wall adjacent cells, and the sensitivity of the results to the thickness of these cells is one of the test criteria that were used to discriminate between the alternative treatments.

Forced and Mixed Convection Pipe Flow

The first case considered is fully developed isothermal pipe flow. The mean velocity profile in conventional wall-law coordinates is shown in Fig. 4 for two Reynolds numbers. At the higher Reynolds number of 10^5 the predicted near-wall velocity falls on the log-law line $U^+ = 2.4 \ln y^+ + 5.45$ irrespective of the thickness of the wall-adjacent cell. The near-wall cell size y_e^* is roughly three times the corresponding value of y_e^+, and it can thus be appreciated that for the case of $y_e^* = 50$ most of the near-wall cell lies within the viscous sublayer. When the bulk Reynolds number falls below 10^4 the additive constant in the log-law relationship is known to increase. Figure 4 shows the experimental data of Kudva & Sesonske (1972) for Re=6753 with which the low-Reynolds-number k-ε model is in very close accord. It should be noted that with the new wall functions, good agreement is also obtained: the inclusion of F_ε to mimic laminarization effects allows the upward displacement of the velocity profile above the "universal" log-law to be captured, and the results are still independent of the size of the near-wall cell.

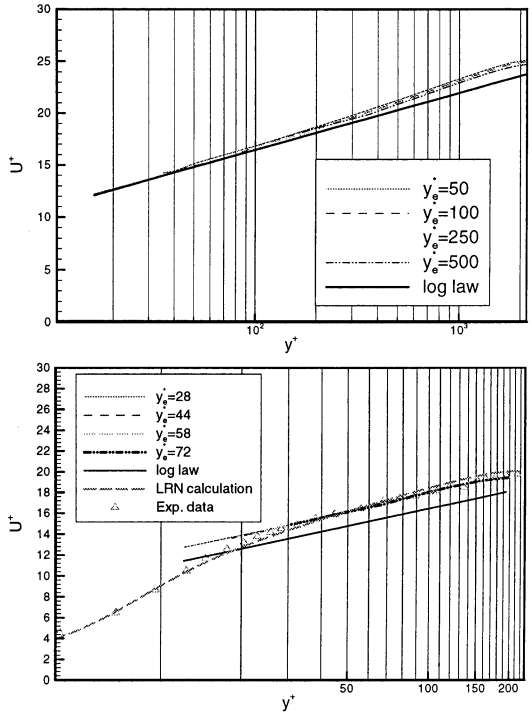

Figure 4: Velocity profiles in fully developed pipe flow at $Re = 10^5$ (upper graph) and $Re = 6753$ (lower graph).

Figure 5 relates to mixed convection in a vertical pipe. Due to the wall heating, the near-wall fluid receives a buoyant upthrust, causing a local velocity maximum and a rapid decrease of shear stress with distance from the wall. This leads to a thickening of the viscous sublayer and a reduction of Nusselt number below that found in fully developed forced convection pipe flow (the Dittus-Boelter correlation denoted by the horizontal line). As noted by Cotton & Jackson (1987), the low-Reynolds-number k-ε model is quite successful at capturing this phenomena, and can be seen to be in good agreement with the data of Li (1994). The new wall func-

tion treatment is also seen to return values close to the experimental data, again with little influence of the near-wall cell size. The close agreement between the wall functions and low-Reynolds-number model results has been verified over a far wider range of conditions than those for which experiments exist. Figure 5 also shows, for example, a situation at an inlet Reynolds number of nearly 10^5 and Grashoff number of 3.46×10^9 where the Nusselt number is reduced to only 40% of that found in forced convection. Again the wall function results are impressively close to those of the low-Reynolds-number model.

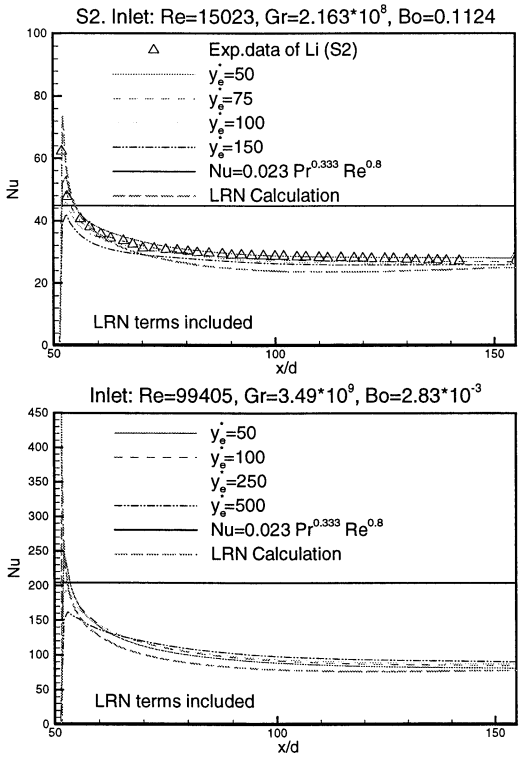

Figure 5: Nusselt number for mixed convection in upward flow in a heated pipe at $Re = 1.5 \times 10^4$, $Gr = 2.2 \times 10^8$ (upper graph) and $Re = 10^6$, $Gr = 3.49 \times 10^9$ (lower graph).

Flow through Asymmetric Plane Diffuser

The next test case, that of separated flow through a diffuser, is one where, due to the significant streamwise curvature associated with separation and reattachment, the flow is not adequately described by a linear eddy-viscosity model in the main flow – indeed, with the low-Reynolds-number form separation does not even occure. However, separation is predicted if one adopts the non-linear eddy-viscosity model of Craft et al (1996). Figure 6 shows the behaviour with this model in three versions: the original low-Reynolds-number form; used in conjunction with the standard wall function, and with the proposed wall function. It must be said that the implementation of this last model is not yet complete as the quantity F_ε takes the value unity since τ_v is greater than τ_w. Evidently the form currently adopted in eq. (14) needs to be adjusted to allow F_ε to take values less than unity in cases where the shear stress rises with distance from the wall. Nevertheless, even with the present form a modest improvement is achieved compared with the usual log law.

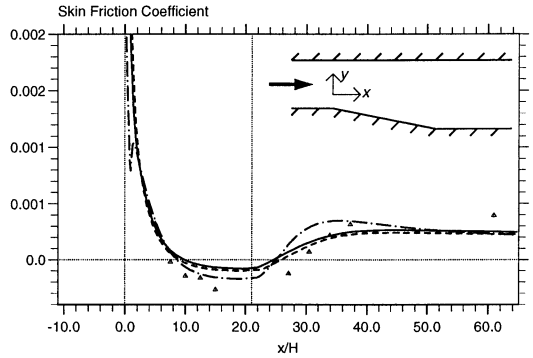

Figure 6: Skin friction coefficient along the diverging wall of the diffuser using different near wall treatments with the linear k-ε model (upper graph) and non-linear EVM (lower graph). — - — Low-Reynolds-number model; —— Standard wall function; - - - New wall function.

Opposed Wall Jet

The final test case is an isothermal, downward directed wall jet measured by Jackson et al (2000) and shown in Fig. 7. This is a preliminary test case for future applications where the wall jet will be hotter than the very slow moving upward bulk flow. The present wall function results have again only been obtained for the case where F_ε is unity. Nevertheless, Fig. 8 shows that the contours of turbulent kinetic energy obtained with the new analytical wall functions are considerably closer to those of the low-Reynolds-number model than is achieved by the standard wall-function prescription.

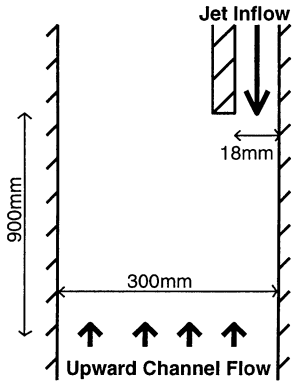

Figure 7: The opposed wall jet flow.

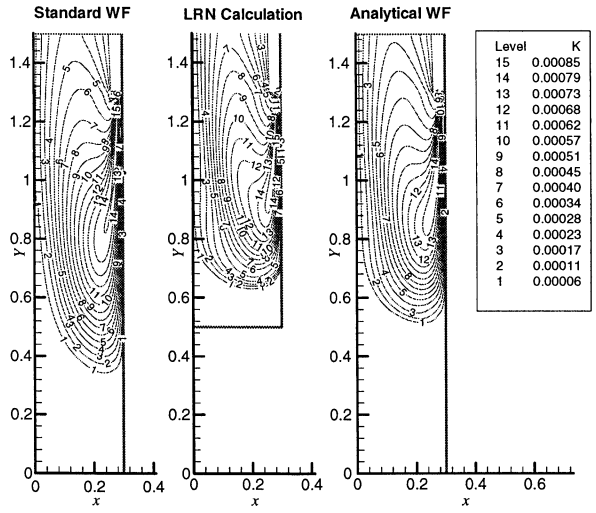

Figure 8: Predicted distribution of the turbulent kinetic energy in the opposed wall jet, using the linear k-ε model with different wall treatments.

CONCLUDING REMARKS

The present analytical wall functions have achieved a useful broadening of the range of near-wall turbulent flows that can be computed without providing a detailed and expensive resolution of the near-wall sublayer. Use of the schemes reduces the overall computing time required by between one and two orders of magnitude compared with a conventional low-Reynolds-number model.

For the first time a wall function approach can be used to compute mixed as well as forced-convection, with little sensitivity of the results to the size of the near-wall cell. The initial application of the scheme to the diffuser and opposed wall jet flows have also shown promising improvements over the use of standard wall functions.

Although these preliminary results are encouraging, a wider programme of tests still needs to be carried out. It is also recognized that further refinements to the modelling need to be introduced, for example to account for the thermal behaviour of liquids with very high or very low Prandtl number. The work is made available at this stage in the hope that other groups may wish to assist in the testing and refinement programme.

Acknowledgements

Different aspects of the work have received financial support from British Energy plc, and from the European Community Brite-Euram III programme. AVG also acknowledges the support of a UK ORS scholarship. Authors' names are sequenceed alphabetically.

References

Chieng, C.C., Launder, B.E. 1980, *Numerical Heat Transfer*, Vol. 3, pp. 189-207.

Cotton, M.A., Jackson, J.D. 1987, "Calculation of turbulent mixed convection in a vertical tube using a low-Reynolds-number k-ε turbulence model", *Proc. 6th Turbulent Shear Flows Symposium*, Toulouse.

Craft, T.J., Launder, B.E., Suga, K. 1996, *Int. J. Heat and Fluid Flow*, Vol. 17, pp. 108-115.

Craft, T.J., Gerasimov, A.V., Iacovides, H., Launder, B.E. 2001, "Progress in the generalization of wall-function treatments", *Proc. 3rd Engineering Foundation Heat Transfer Conference*, Alaska.

George, W.K., Capp, S.P. 1979, *Int. J. Heat Mass Transfer*, Vol. 22, pp. 813-826.

Gerasimov, A.V. 2001, "Development of a new analytical wall-function approach for modelling mixed convection phenomena", *Report BWD 40029343*, Mech. Eng. Dept., UMIST, Manchester, UK.

Jackson, J.D., He, S., Xu, Z., Wu, T. 2000, "CFD quality and trust - generic studies of thermal convection", *Report HTH/GNSR/5029*, School of Engineering, University of Manchester, UK.

Johnson, R.W., Launder, B.E. 1982, *Numerical Heat Transfer*, Vol. 5, pp. 493-496.

Jones, W.P., Launder, B.E. 1972, *Int. J. Heat Mass Transfer*, Vol. 15, pp. 301-314.

Kudva, A.A., Sesonske, A. 1972, *Int. J. Heat Mass Transfer*, Vol. 15, p. 127.

Li, J. 1994, "Studies of buoyancy-influenced convective heat transfer to air in a vertical tube", PhD Thesis, University of Manchester, UK.

Obi, S. Aoki, K, Masuda, S. 1993, "Experimental and computational study of turbulent separating flow in an asymmetric plane diffuser", *Proc. 9th Turbulent Shear Flows Symposium*, Kyoto.

Patankar, S.V., Spalding, D.B. 1972, *Int. J. Heat Mass Transfer*, Vol. 15, p. 1787.

Spalding, D.B. 1967, "Monograph on turbulent boundary layers", *Technical Report TWF/TN/33*, Dept. of Mech. Eng., Imperial College of Science and Technology, London.

Wolfshtein, M. 1969, *Int. J. Heat Mass Transfer*, Vol. 12, pp. 301-318.